

Thermal neutron flux evaluation by a single crystal CVD diamond detector in LHD deuterium experiment

**Makoto Kobayashi^{a,b}, Kunihiro Ogawa^{a,b}, Mitsutaka Isobe^{a,b}, Takeo Nishitani^a,
Shuji Kamio^a, Yutaka Fujiwara^a, Tomomi Tsubouchi^{c,b}, Sachiko Yoshihashi^d,
Akira Uritani^d, Minoru Sakama^e, Masaki Osakabe^{a,b}, and the LHD Experiment
Group^a**

^a*National Institute for Fusion Science, National Institutes of Natural Sciences,
322-6 Oroshi, Toki, Gifu, Japan.*

^b*SOKENDAI (Graduate University for Advanced Studies),
322-6 Oroshi, Toki, Gifu, Japan.*

^c*National Institute for Basic Biology, National Institutes of Natural Sciences,
38 Nishigonaka, Myodaiji, Okazaki, Aichi, Japan.*

^d*Nagoya University,
Furo-cho, Chikusa-ku, Nagoya, Aichi, Japan*

^e*Tokushima University
2-24, Shinkura-cho, Tokushima, Japan.*

E-mail: kobayashi.makoto@nifs.ac.jp

ABSTRACT: The single crystal CVD diamond detector (SDD) was installed in the torus hall of the Large Helical Device (LHD) to measure neutrons with high time resolution and neutron energy resolution. The LiF foil with 95.62 % of ⁶Li isotope enrichment pasted on the detector was used as the thermal neutron convertor as the energetic ions of 2.0 MeV alpha and 2.7 MeV triton particles generated in LiF foil and deposited the energy into SDD.

SDD were exposed to the neutron field in the torus hall of the LHD during the 2nd campaign of the deuterium experiment. The total pulse height in SDD was linearly proportional to the neutron yield in a plasma operation in LHD over 4 orders of magnitude. The energetic alpha and triton were separately measured by SDD with LiF with the thickness of 1.9 μm, although SDD with LiF with the thickness of 350 μm showed a broadened peak due to the large energy loss of energetic particles generated in the bulk of LiF. The modeling with MCNP and PHITS codes well interpreted the pulse height spectra for SDD with LiF with different thicknesses. The results above demonstrated the sufficient time resolution and energy discrimination of SDD used in this work.

KEYWORDS: diamond detector; neutron; MCNP; PHITS.

Contents

| | |
|--|----------|
| 1. Introduction | 1 |
| 2. Single crystal CVD diamond detector | 2 |
| 3. Particle transport modeling | 2 |
| 4. Neutron irradiation in the torus hall of LHD | 3 |
| 5. Results and discussion | 3 |
| 6. Conclusion | 5 |

1. Introduction

In the fusion experimental devices using deuterium and/or tritium plasma, the neutron detector with high time resolution, measureable for the fast neutron under thermal and epithermal neutrons and gamma-ray background environment, and capable a stable operation is desired for the diagnostics of fusion plasma where high density and high temperature plasma produces a high neutron flux [1-3]. Also, the neutron activation in the components in the torus hall is one of the issues from the point of view of safety. The cross-sections of activation reactions between neutron and elements in the components largely depend on the neutron energy. Also, radioactive isotopes emit radiation such as gamma-ray, thus restricting the maintenance work due to the occupational radiation exposure for workers. Therefore, the advanced neutron detector capable of discriminatively measuring fast, epithermal, thermal neutrons as well as gamma-ray can accelerate physics research and secure radiation safety in the experiment.

For these requirements, one of the solutions is to adopt the single crystal diamond (s-diamond). The s-diamond is one of the semiconductor materials. The energy deposited from the radiation into s-diamond creates the hole-electron pairs. By the bias voltage applied on each surface of s-diamond, the hole-electron pairs oppositely penetrate through the bulk of s-diamond. Therefore, one can evaluate the radiation dose as the current which was carried by the hole-electron motion. The s-diamond detector (SDD) has advantages such as the tolerance for radiation dose, the high operation temperature, small size, and fast neutron measurement capability [4]. In addition, the pasting of foils consisting of lithium or boron on the s-diamond can provide SDD with the ability for the measurement of thermal and epithermal neutrons [5]. The energetic ions generated by the nuclear reactions of thermal and epithermal neutrons with lithium and boron such as ${}^6\text{Li}(n,\alpha){}^3\text{H}$ and ${}^{10}\text{B}(n,\alpha){}^7\text{Li}$ reactions, respectively, have large energies around 1 MeV or more [6]. Then, the incident energetic ions transfer their energy into s-diamond. Therefore, the measurement of thermal and epithermal neutrons can be implemented.

The Large Helical Device (LHD) is one of the largest superconducting fusion experimental devices. The deuterium experiments in LHD began in 2017 to obtain the high-performance plasma in helical type fusion device [7-9]. Side by side with physics research, the large volume of the LHD and its torus hall can provide a wide range of neutron flux with various neutron energies, which are available for the other research fields such as medical and biology research.

Therefore, an SDD was installed into the torus hall of LHD in the 2nd campaign of the deuterium experiment. The lithium fluoride (LiF) foil was used as the thermal neutron convertor. The signals from SDD were processed into the pulse height spectrum (PHS) to evaluate the sensitivity, energy resolution, and time resolution of SDD.

2. Single crystal CVD diamond detector

The SDD used in this study was purchased from Cividec instrumentation GmbH. The s-diamond was fabricated by the chemical vapor deposition (CVD). The size of the s-diamond is 4.5 mm × 4.5 mm, and the thickness is 140 μm. The contact titanium electrode is pasted on both sides of s-diamond. The s-diamond is in housing with the size of 54 mm × 10 mm × 8 mm made of polychlorinated biphenyl (PCB). There is a window with the size of 2.5 mm^φ in the housing in front of one side of the s-diamond to allow the energetic ions to implant into the s-diamond directly. The lid of the window is the size of 54 mm × 10 mm × 1 mm. The LiF foil is pasted on a surface of the lid. The size of the LiF foil is 4 mm^φ, which is sufficiently larger than that of the window in the housing. LiF foil was synthesized with the isotope enrichment of ⁶Li as 95.62 % to increase the sensitivity for thermal neutron. In the measurement, a side of the lid with the LiF foil faced to the s-diamond through the window in the housing. The distance between the LiF foil and the s-diamond is 1 mm. The photograph of the SDD and the lid is shown in Fig. 1. In this study, two types of LiF foil with different thicknesses as 1.9 μm and 350 μm were used to evaluate the influence of energy loss of energetic ions in the LiF foils on the SDD signal.

In the measurement, SDD was sealed into the ICF-34 metal flange to restrict the tritium release. Then, bias voltage of -120 V was applied to a surface of the SDD through the pre-amplifier (HV broadband Amplifier) of Cividec instrumentation GmbH. The signal from SDD was acquired by fast processing ADC and FPGA. The sampling rate of this system was 1 GHz.

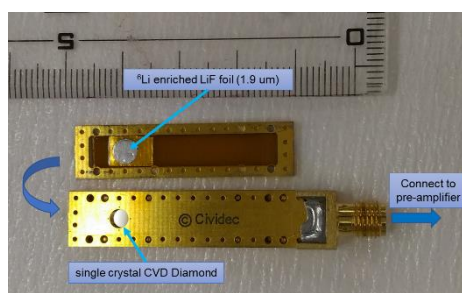


Figure 1. SDD and the lid pasted with LiF foil with the thickness of 1.9 μm

3. Particle transport modeling

The count rate of energetic ions (alpha and triton) by the SDD depends not only on the neutron flux and neutron energy, but also on the transport processes of energetic ions in the LiF foil. Therefore, the neutron transport in the torus hall and the secondary energetic ion transport in the SDD must be calculated. In this study, MCNP6 (General Monte Carlo N-Particle code) was applied for the neutron transport calculation in the LHD torus hall [10]. Then, the transport processes of energetic ions in SDD, including generation, energy loss in LiF foil, and energy deposition into s-diamond, were calculated by PHITS (Particle and Heavy Ion Transport code System) [11].

The neutron transport model for MCNP6 calculation has been developed for LHD [12]. The model includes the torus hall, LHD body, coils, support structure. By using the cell tally in MCNP6, the neutron energy spectrum at the position of SDD could be evaluated.

The transport calculation for energetic ions was conducted by PHITS with using the neutron energy spectrum evaluated by MCNP6 calculation. For the calculation in PHITS, the SDD was carefully modeled. Then, two plane neutron sources were set from the opposite direction to the SDD. The size of the plane neutron source was 4.5 mm × 4.5 mm, which is sufficiently larger than that of s-diamond and LiF foil. Neutrons irradiated into the surface normal of the LiF foil

and the s-diamond. These neutron sources have the same neutron energy spectrum evaluated by MCNP6 calculation. The event generator mode was applied to precisely evaluate the energy and the momentum of energetic ions generated by the nuclear reaction. The averaged count as a function of deposited energy into SDD in a single event was estimated by T-deposit tally. For this tally, the statistical dispersion on the deposited energy as gaussian distribution was assumed. Also, the trigger level was imitated by setting the cut-off energy. In this work, the cut-off energy was set at around 300 keV.

4. Neutron irradiation in the torus hall of LHD

In LHD, plasma operation with deuterium induces ${}^2\text{H}(d,p){}^3\text{H}$ and ${}^2\text{H}(d,n){}^3\text{He}$ reactions. The cross-sections for these reactions are almost the same. The latter reaction produces neutron with the energy of 2.45 MeV. The former reaction produces triton. A part of triton generated in the plasma subsequently reacts with deuterium with ${}^3\text{H}(d,n){}^4\text{He}$ reaction which emits the 14.1 MeV neutron. This reaction is called a triton burn-up reaction, and 0.05-0.4 % of triton induces this reaction in a plasma operation [13,14]. Consequently, neutrons originated from 2.45 MeV (dominant) and 14.1 MeV (minor) are transported in the torus hall.

The SDD was installed into the torus hall of LHD. The position of SDD was underneath the 9.5L port of LHD, and placed near the floor level, corresponding to the distance of 5.5 m from the plasma. The signal from the SDD was transferred to the DAQ system in the basement of the torus hall. The binary file made from the measurement data was processed by the python numpy module.

The signal from the SDD was obtained in each plasma operation (shot) in LHD. The PHS was acquired by the integration of a pulse height of signals. The neutron yield was different in each plasma shot, and monitored by the neutron flux monitor (NFM). The SDD with the 1.9 μm -thick LiF foil was exposed to neutron in the plasma shot number of #147425-#147820. That with 350 μm -thick LiF foil was placed in the torus hall during the plasma shot number of #147886-#148459.

5. Results and discussion

Fig. 2 shows ten typical signals from SDD with 1.9 μm -thick LiF during deuterium plasma shot. The signals were observed within about 10 ns. The shapes of the signal were almost the same for SDD with LiF with the thicknesses of 1.9 and 350 μm . The signals can be separated into

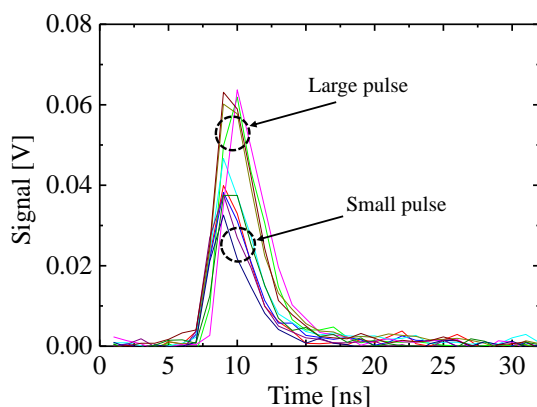


Figure 2. Typical signal from SDD with 1.9 μm LiF

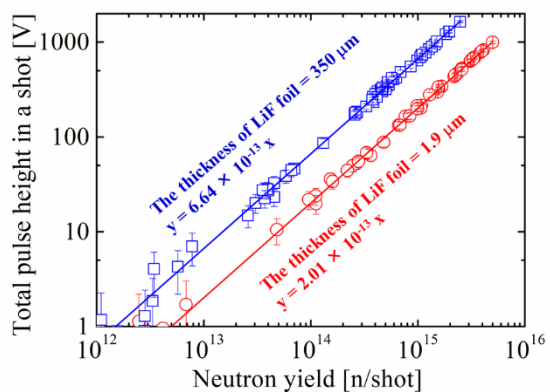


Figure 3. Total pulse height in SDD integrated over a shot as a function of neutron yield

large pulse and small pulse. In the nuclear reaction of ${}^6\text{Li}(n,\alpha){}^3\text{H}$, the recoil energies of alpha and triton particles are around 2.0 MeV and 2.7 MeV, respectively. Also, these particles recoil in the opposite direction of each other. Hence, when either particle injects into s-diamond, another particle implants into the lid of SDD. Consequently, the large pulse should correspond to the deposition of triton. The small pulse would be caused by alpha particle.

The total pulse height integrated over a deuterium plasma shot is displayed in Fig. 3 as a function of the neutron yield in each plasma shot. The linear relationship between the total pulse height and the neutron yield in the wide neutron yield ranging from 10^{12} - 10^{16} n/shot was obtained. This result indicates that the counting loss of SDD was quite small in this experimental condition. The total pulse height for SDD with 350 μm -thick LiF was almost 3.3 times as large as that with LiF with the thickness of 1.9 μm . Compared with thinner LiF foil, the thicker LiF foil can produce more energetic ions, even larger energy loss of energetic ions in the foil, resulting in the higher count rate in SDD.

The PHS for SDD with 1.9 μm -thick LiF and 350 μm -thick LiF are shown in Fig. 4. Note that the count in perpendicular axis in Fig. 4 is normalized by the neutron yield. A broadend peak was found in the case with 350 μm -thick LiF. Besides, in the case with 1.9 μm -thick LiF, two peaks at around 0.15 V and 0.26 V were observed. According to Fig. 2, the peak at 0.15 V was assigned to alpha particle. The peak at 0.26 V was attributed to triton. Also, the peak areas for triton was two times larger than that by alpha particle even though the same number of alpha and triton generated in the LiF foil. This difference would be caused by the energy loss efficiency of these energetic ions in the LiF foil.

The PHS estimated by PHITS code in the cases for SDD with 1.9 μm -thick LiF and 350 μm -thick LiF are shown in Figs. 5 (a) and (b), respectively. Compared with Fig. 4, PHITS code successfully reproduced the PHS for these two cases observed in the experiment. The peak areas in the case with 350 μm -thick LiF was about 3.5 times as large as that in the case with 1.9 μm -thick LiF foil. This is consistent with the difference in the relation of total pulse height integrated over a deuterium plasma shot as a function of the neutron yield in each shot as shown in Fig. 2.

The peak position of triton in Fig. 5 (a) was located at 2.7 MeV corresponding to the primitive recoil energy of triton in ${}^6\text{Li}(n,\alpha){}^3\text{H}$ reaction. However, the peak position for alpha particle was around 1.5 MeV, which is lower than the virgin recoil energy of alpha particle generated in ${}^6\text{Li}(n,\alpha){}^3\text{H}$ reaction. In addition, in Fig. 5 (b), the dominant contribution on the PHS for SDD is from triton. This means that most of alpha particles could not penetrate through the LiF foil with the thickness of 350 μm . These results can be caused by the difference in the energy

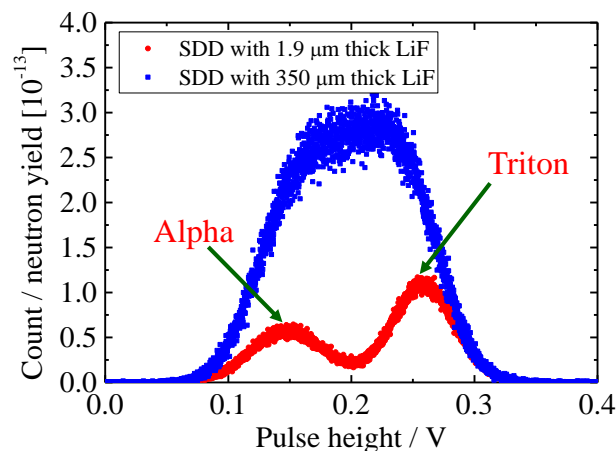


Figure 4. Pulse height spectra for SDD with LiF with different thicknesses.

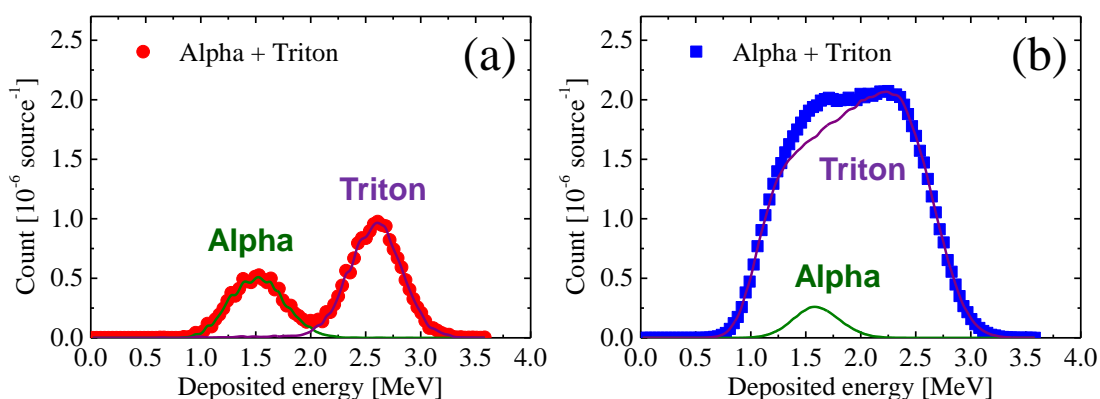


Figure 5. The PHS of SDD with (a) 1.9 μm LiF and (b) 350 μm LiF estimated by PHITS.

loss efficiency between 2.0 MeV alpha and 2.7 MeV triton in LiF foil. Because of the larger positive charge and the mass of alpha particle, the energy loss of alpha particle is larger than that of triton. Of course, triton is also influenced by the energy loss process in LiF. Therefore, in Fig. 5 (b), the peak was broadened due to the wide range of the rest of the energy in triton which depends on the depth of LiF where the triton was generated. According to the PHS evaluated by PHITS, one can estimate the thermal neutron flux at the position of the SDD in the torus hall of LHD. Consequently, the thermal neutron flux of $1.0 \times 10^{-8} \text{ n cm}^{-2} \text{ s}^{-1}$ for single neutron source was obtained. This value is consistent with our previous research with using activation foil method [15].

The exposure of the SDD with LiF foil to the neutron field in the torus hall of the LHD during deuterium experiment showed the sufficient time resolution and energy resolution of SDD in the measurement of thermal neutron. However, fast neutrons were hardly detected in this work, although the fast neutron detection capability is the typical advantages of SDD. One of the reasons of this result should be a low flux of fast neutron capable to induce $^{12}\text{C}(n,\alpha)^9\text{Be}$ reaction because this reaction requires the threshold neutron energy above 7 MeV [6]. Only neutrons generated by $^3\text{H}(d,n)^4\text{He}$ reaction can overcome this threshold energy although the triton burn-up ratio is small. Also, the low cross-section of $^{12}\text{C}(n,\alpha)^9\text{Be}$ reaction [16], a small size of SDD, and the far distance between the SDD and the plasma, are other reasons. The modification of SDD position as well as the enlargement of the SDD size are planned for the next deuterium experiment campaign.

6. Conclusion

In this study, the single crystal CVD diamond detector (SDD) was installed into the torus hall of LHD to measure neutron with high time resolution and neutron energy resolution. The LiF foils were affixed to the detector was used as the thermal neutron convertor into the energetic ions of alpha and triton particles. A good linearity between the total pulse height in SDD and the neutron yield in a plasma operation in LHD were observed. The energetic alpha and triton were separately measured by SDD with LiF with the thickness of 1.9 μm , although SDD with LiF with the thickness of 350 μm showed a broadened peak. The modeling with MCNP and PHITS codes well interpreted the pulse height spectra for SDD with LiF with different thicknesses.

Acknowledgments

This work is supported by the NINS program for cross-disciplinary study (Grant Number 0131190), the NIFS Collaboration Research Program (NIFS19KOAA001), and LHD project budget.

References

- [1] M. Ishikawa et al., First measurement of neutron emission profile on JT-60U using Stilbene neutron detector with neutron-gamma discrimination, *Rev. Sci. Instrum.* **73** (2002) 4237.
- [2] P.V. Belle et al., Calibration of the JET neutron yield monitors using the delayed neutron counting technique, *Rev. Sci. Instrum.* **61** (1990) 3178.
- [3] Z. Stancar et al., Generation of a plasma neutron source for Monte Carlo neutron transport calculations in the tokamak JET, *Fusion Eng. Des.*, **136** (2018) 1047-1051.
- [4] V.D. Lovalchuk et al., Diamond detector as fast neutron spectrometer, *Nucl. Instrum. Meth. Phys. Res. A*, **351** (1994) 590-591.
- [5] S. Alaviva et al., Thermal and fast neutron detection in chemical vapor deposition single-crystal diamond detectors, *Rev. Sci. Instrum.* **103** (2008) 054501.
- [6] K. Shibata, et al, JENDL-4.0: A New Library for Nuclear Science and Engineering, *J. Nucl. Sci. Technol.* **48** (2011) 1-30.
- [7] Y. Takeiri, The Large Helical Device: entering deuterium experiment phase toward steady-state helical fusion reactor based on achievements in hydrogen experiment phase, *IEEE T. Plasma Sci.*, **46** (2018) 2348-2353.
- [8] A. Komori, et al., Goal and achievements of Large Helical Device project, *Fusion Sci. Technol.*, **58** (2010) 1-11.
- [9] Y. Takeiri, et al, Extension of the operational regime of the LHD towards a deuterium experiment, *Nucl. Fusion*, **57** (2017) 102023.
- [10] X-5 Monte Carlo Team, MCNP User's Guide - Code Version 6.1.1beta, LA-CP-14-00745 (Los Alamos National Laboratory, Los Alamos, 2014).
- [11] T. Sato et al., Features of Particle and Heavy Ion Transport code System (PHITS) version 3.02, *J. Nucl. Sci. Technol.*, **55** (2018) 684-690.
- [12] T. Nishitani, et al., Monte Carlo simulation of the neutron measurement for the Large Helical Device deuterium experiments, *Fusion Eng. Des.*, **123** (2017) 1020-1024.
- [13] N. Pu et al., Initial results of triton burnup study in the Large Helical Device, *Plasma. Fusion. Res.*, **13** (2018) 3402121.
- [14] K. Ogawa et al., Energetic-ion confinement studies by using comprehensive neutron diagnostics in the Large Helical Device, accepted to *Nucl. Fusion*.
- [15] M. Kobayashi et al., First measurements of thermal neutron distribution in the LHD torus hall generated by deuterium experiments, *Fusion Eng. Des.*, **137** (2018) 191-195.
- [16] T. Shimaoka et al., A diamond 14 MeV neutron energy spectrometer with high energy resolution, *Rev. Sci. Instrum.* **87** (2016) 023503.